Prediction of unsteady flow over airfoils using a quasi-simultaneous interaction method

H.A. Bijleveld
ECN Wind Energy
P.O.Box 1, 1755 ZG Petten, the Netherlands
e-mail: bijleveld@ecn.nl

A.E.P. Veldman
Institute of Mathematics and Computing Science
University of Groningen
P.O.Box 407, 9700 AK Groningen, the Netherlands
e-mail: a.e.p.veldman@rug.nl

Abstract

The unsteady flow over airfoils is determined by splitting the flow field into a viscous and inviscid region. Interaction between these two regions is established by applying the strong quasi-simultaneous interaction method of Veldman [11]. In this method, the boundary-layer is solved together with the interaction law after which an inviscid calculation is carried out. For laminar and turbulent boundary-layer flows over two-dimensional dented plates it is shown analytically and numerically that the quasi-simultaneous interaction method removes the singularity at separation. Also, using either primary or characteristic variables in the sets of equations in simulations yields the same result. This means that the determination and use of characteristic directions of the viscous flow is feasible in the method ROTORFLOW 2D which is developed by ECN Wind Energy.

1 Introduction

The growth in size of wind turbines and their blades requires more accurate prediction methods for the determination of aerodynamic loads. Current methods for predicting aerodynamic loads on wind turbine blades use engineering models and a steady approach of the flow field like e.g. BEM (Blade-Element Momentum) methods and XFOIL [2]. On the other hand, carrying out a full Navier-Stokes simulation of the flow field (e.g. RANS) can give higher accuracy of the prediction, but it consumes too much computational time to be a practical design tool.

The goal of ROTORFLOW 2D, being a part of the ROTORFLOW project of ECN Wind Energy, is to create a wind turbine rotor aerodynamics simulation code that requires little user expertise and computational effort, but can compute in detail the unsteady aerodynamic characteristics of rotor airfoils. The simulation of separated flows will be feasible.

The method ROTORFLOW 2D will be a combination of a panel method flow solver for the 2D, unsteady, incompressible, inviscid external flow and an integral boundary-layer solver for the 2D unsteady, viscous flow near the blade surface [8], see Figure 1. The strong interaction between these two flow regions in separated flows will be accounted for by a so-called viscous-inviscid interaction method. The interaction method ensures the exchange between the integral boundary-layer variables of the viscous flow and the inviscid flow variables. This method has extensively been applied in airfoil applications (e.g. [10]), but is hardly used in the design of wind turbine blades. Here we will focus on the interaction method.

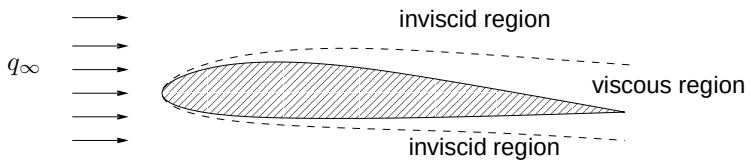

Figure 1: Domain decomposition into a viscous and inviscid region. Interaction takes place at the dashed line. q_∞ represents the inflow field.

The viscous region of Figure 1 is modeled as a boundary-layer. A boundary-layer is a very thin region near the surface where the viscous effects are significant. In the region near the surface of the airfoil the effects of viscosity slow the flow down from the outher edge of this so-called boundary-layer to zero velocity at the surface. The edge of the boundary-layer is often defined as the point where the tangential velocity reaches approximately 99% of the external flow. In this work we will use integral boundary-layer equations[1]. The variables of interest are the velocity at the edge of the boundary-layer (u_e), the displacement thickness (δ^*), momentum thickness (θ) and the shape factor (H).

This paper focusses on the application of the strong quasi-simultaneous interaction method. First, the interaction method will be introduced and its features explained. This is followed by the description of the implementation of the interaction method. The paper ends by showing some preliminary results of the implementation of the method for flows over flat and dented plates.

2 Viscous-Inviscid Interaction Methods

The philosophy of viscous-inviscid interaction methods is that it exchanges the velocity vector and the boundary-layer displacement thickness - modeled via a transpiration velocity - between the inviscid and viscous region until a matching solution between the two regions is obtained.

Mathematically, the phenomenon of interaction can be described as follows:

$$\begin{cases} \vec{u}_e &= E\delta^* \\ \vec{u}_e &= B\delta^* \end{cases}, \tag{1}$$

with E and B the set of external flow and integral boundary-layer equations respectively.

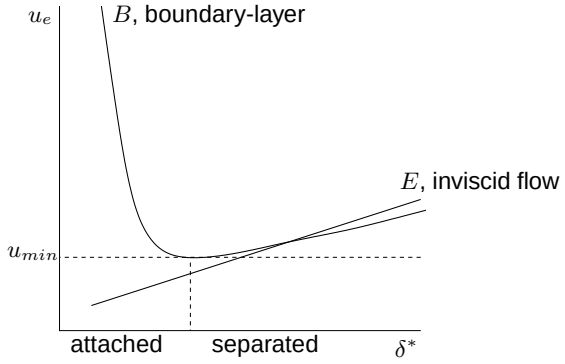

Figure 2: Schematic representation of the relation between u_e and δ^* for B and E.

In Figure 2 the relations between u_e and δ^* for the viscous and inviscid flow are drawn schematically where for convenience the inviscid flow relation is supposed to be linear. The aim of any viscous-inviscid interaction method is to ensure a connection between the solution of the flow domains. This is achieved if E has a slope that is positive enough to have an intersection with the curve of B.

Since the development of the first viscous-inviscid interaction methods, several types of interaction methods have been developed. Four basic types of interaction methods will be discussed here.

The most straightforward method is the direct method. In this method, see Figure 3a, the viscous and inviscid regions are calculated subsequently:

$$\begin{cases} \vec{u}_e^{(n)} &= E\delta^{*(n-1)} \\ \delta^{*(n)} &= B^{-1}\vec{u}_e^{(n)} \end{cases}, \tag{2}$$

where n is the iteration number. This method works well for attached flows where the effect of the boundary-layer on the external flow is small. However, at the point of separation a singularity occurs and B^{-1} cannot be determined. This is the well-known Goldstein singularity [4]. This can also be

[1] See e.g. [9] for an explanation on boundary-layers

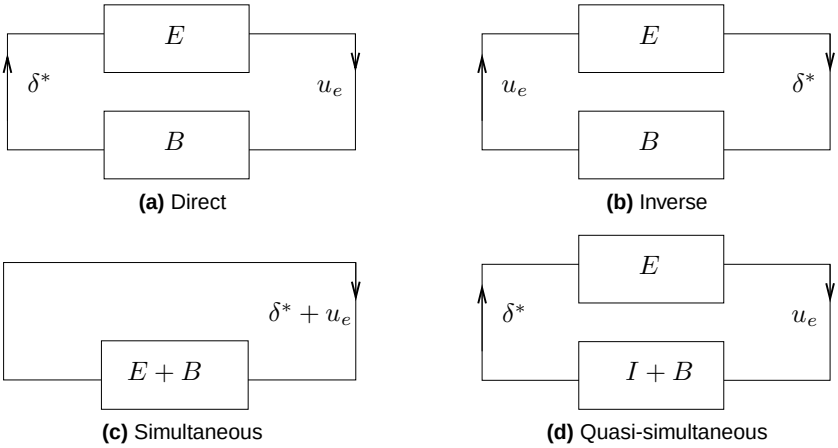

Figure 3: Four basic types of interaction methods.

learned from Figure 2 as for not every u_e a corresponding δ^* can be found in the boundary-layer model. Figure 2 shows that the minimum of the B-curve is at the point of separation.

Solving the boundary-layer equations with a known displacement thickness instead of a known velocity is an inverse method (Figure 3b):

$$\begin{cases} \delta^{*(n)} & = E^{-1}\vec{u}_e^{(n-1)} \\ \vec{u}_e^{(n)} & = B\delta^{*(n)} \end{cases}. \tag{3}$$

Catherall and Mangler [1] first proposed this method and this method is able to calculate separated flows. The convergence of the interaction scheme is slow, however.

The direct and inverse method assume a hierarchy between the flow regimes and are so-called weak interaction methods. Avoiding this hierarchy can be achieved by solving the viscous and inviscid flow simultaneously (Figure 3c):

$$\begin{cases} \vec{u}_e^{(n)} - E\delta^{*(n)} & = 0 \\ \vec{u}_e^{(n)} - B\delta^{*(n)} & = 0 \end{cases}. \tag{4}$$

This is a robust method and calculates separated flow well. The XFOIL code of Drela is based on this idea [2]. However, a drawback of this method is that the equations for both flows are modeled in one system of equations, reducing the flexibility in flow modeling and increasing software complexity.

Veldman [11] combined the advantages of the direct and simultaneous method in the quasi-simultaneous interaction scheme, see Figure 3d and Figure 4. This method solves the viscous flow region together with an *approximation* (indicated with I) of the external flow and subsequently solves the inviscid flow:

$$\begin{cases} \vec{u}_e^{(n)} - I\delta^{*(n)} & = E\delta^{*(n-1)} - I\delta^{*(n-1)} \\ \vec{u}_e^{(n)} & = B\delta^{*(n)} \end{cases} \Rightarrow (I-B)\delta^{*(n)} = (I-E)\delta^{*(n-1)}, \tag{5}$$

where I is the approximation of the external flow which is called *interaction-law*. The interaction-law is formulated such that it has no influence on the converged solution: when $\delta^{*(n)} = \delta^{*(n-1)}$, I cancels from equation (5). In Figure 4 the interaction-law is sketched together with the inviscid and boundary-layer relations. The interaction-law is formulated such that it always has an intersection with B even in cases where E might not intersect.

In the past, several interaction-laws have been applied, see for example Edwards [3] and Van der Wees and Van Muijden [10]. The interaction-law applied in this work is based on the quasi-simultaneous interaction-law formulation of Veldman [12] and will be discussed in the next section.

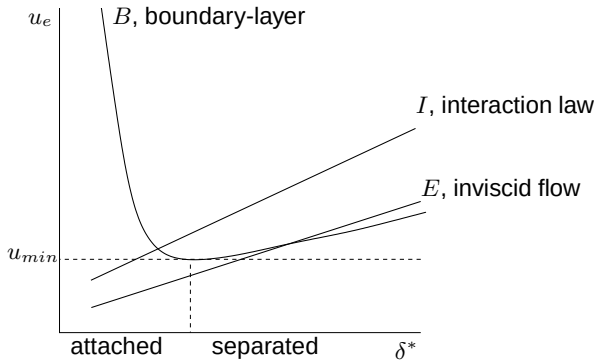

Figure 4: Schematic representation of the relation between u_e and δ^* for B, E and I.

3 Interaction-law

In the quasi-simultaneous method, the interaction-law I is applied. The interaction-law represents a simplification of the external flow such that only the essentials of the inviscid flow are taken into account. The resulting strong interaction method closely resembles a direct method, with the added advantage that separated flow can be calculated.

For the formulation of the interaction-law equation, only the local influence of the external flow on the boundary-layer is taken into account. This results in a very simple algebraic expression for the interaction-law:

$$I: \; u_e - cq_\infty \delta^* = \mathrm{RHS}, \tag{6}$$

with c the interaction-law coefficient and q_∞ the absolute value of the inflow velocity. The right-hand side contains information of the external flow. As long as the interaction-law coefficient is chosen positive enough, the relation I sketched in Figure 4 will have an intersection with B.

For two-dimensional applications the interaction-law equation (6) is, [12]:

$$I_{2D}: \; u_e - \frac{4q_\infty \delta^*}{\pi h} = \mathrm{RHS}, \tag{7}$$

where h is the mesh width from the discretisation of the external flow model.

4 Implementation of interaction in boundary-layer models

In ROTORFLOW 2D the quasi-simultaneous interaction-law introduced in section 3 will be implemented. In this section, the implementation of the quasi-simultaneous interaction method for a two-dimensional laminar and turbulent boundary-layer model will be discussed. We will show that the singularity at separation is removed by the substitution of the interaction-law equation. At the end of the section, the sets of equations will be formulated in a different kind of variables. The equations appearing in the resulting set are decoupled.

4.1 Boundary-layer models

We will consider both laminar and turbulent boundary-layer flow over two-dimensional flat and dented plates. The models that are used are given here.

4.1.1 Laminar model

For the laminar boundary-layer model we use a two-equations model. The von Kárman and mechanical energy equation read respectively:

$$\frac{1}{u_e^2}\frac{\partial u_e \delta^*}{\partial t} + \frac{1}{u_e^2}\frac{\partial u_e^2 \theta}{\partial x} + \frac{\delta^*}{u_e}\frac{\partial u_e}{\partial x} = \frac{C_f}{2}, \tag{8}$$

$$\frac{1}{u_e^3}\frac{\partial u_e^2 \theta}{\partial t} + \frac{1}{u_e}\frac{\partial \delta^*}{\partial t} + \frac{1}{u_e^3}\frac{\partial u_e^3 \delta^k}{\partial x} = C_D. \tag{9}$$

The closure-relations for δ^k, C_f and C_D are those defined by Nishida [7].

4.1.2 Turbulent model

For the turbulent boundary-layer model we use the von Kárman and Head's Entrainment equation ([5], [9]):

$$\frac{1}{u_e^2}\frac{\partial u_e \delta^*}{\partial t} + \frac{\partial \frac{\delta^*}{H}}{\partial x} + \frac{\delta^*}{u_e}(1+\frac{2}{H})\frac{\partial u_e}{\partial x} = \frac{C_f}{2}, \tag{10}$$

$$\frac{1}{u_e}\frac{\partial}{\partial t}\left(\delta^*\left(\frac{H_1}{H}+1\right)\right) + \frac{1}{u_e}\frac{\partial}{\partial x}\left(\frac{H_1 \delta^* u_e}{H}\right) = C_E. \tag{11}$$

The closure model used is from Houwink [6].

4.2 Substitution of interaction-law equation

The two-dimensional interaction-law (eq. (7)) is substituted in the derivatives of the boundary-layer equations of section 4.1. The derivatives of the interaction law with respect to time and space are[2]:

$$\frac{\partial u_e}{\partial t} = c\frac{\partial \delta^*}{\partial t}; \qquad \frac{\partial u_e}{\partial x} = c\frac{\partial \delta^*}{\partial x} + \frac{\partial}{\partial x}\left(u_{ext} - c\delta^*_{ext}\right). \tag{12}$$

The values of u_{ext} and δ^*_{ext} are known from the previous inviscid calculation.

For the laminar case we obtain the following set of boundary-layer equations B_{lam}:

$$B_{lam}: \begin{cases} \frac{1}{u_e}(1+\frac{c\delta^*}{u_e})\frac{\partial \delta^*}{\partial t} + \frac{\partial \theta}{\partial x} + c(2\theta+\delta^*)\frac{\partial \delta^*}{\partial x} = \frac{C_f}{2} + \frac{1}{u_e}(\theta+\delta)\frac{\partial}{\partial x}(u_{ext} - c\delta^*_{ext}) \\ \frac{1}{u_e}\frac{\partial \theta}{\partial t} + \frac{1}{u_e}(1+2\frac{c\theta}{u_e})\frac{\partial \delta^*}{\partial t} + \frac{\partial \delta^k}{\partial x} + 3c\delta^k\frac{\partial \delta^*}{\partial x} = C_D + \frac{3\delta^k}{u_e}\frac{\partial}{\partial x}(u_{ext} - c\delta^*_{ext}) \end{cases} \tag{13}$$

and for the turbulent case B_{turb}:

$$B_{turb}: \begin{cases} \frac{1}{u_e}(1+\frac{c\delta^*}{u_e})\frac{\partial \delta^*}{\partial t} - \frac{\delta^*}{H^2}\frac{\partial H}{\partial x} + \left[\frac{1}{H} + \frac{c\delta^*}{u_e}(1+\frac{2}{H})\right]\frac{\partial \delta^*}{\partial x} = \frac{C_f}{2} + \frac{\delta^*}{u_e}(1+\frac{2}{H})\frac{\partial}{\partial x}(u_{ext} - c\delta^*_{ext}) \\ \frac{1}{u_e}\frac{\partial}{\partial t}\left(\delta^*\left(\frac{H_1}{H}+1\right)\right) + \frac{H_1}{H}\left(1+\frac{c\delta^*}{u_e}\right)\frac{\partial \delta^*}{\partial x} + \frac{\delta^*}{H}\left(\frac{\mathrm{d}H_1}{\mathrm{d}H} - \frac{H_1}{H}\right)\frac{\partial H}{\partial x} = C_E + \frac{\delta^*}{u_e}\frac{H_1}{H}\frac{\partial}{\partial x}(u_{ext} - c\delta^*_{ext}) \end{cases} \tag{14}$$

4.3 Singularity at separation

The quasi-simultaneous interaction method removes the singularity at separation. By expanding the derivatives appearing in the sets of equations B_{lam} and B_{turb}, they can be written in a form like:

$$[P]\frac{\partial \phi}{\partial t} + [Q]\frac{\partial \phi}{\partial x} = \{R\}, \tag{15}$$

with ϕ the vector of unknowns. In the laminar case $\phi = \{\delta^*, \theta\}$ and in the turbulent case: $\phi = \{\delta^*, H\}$.

[2] We assume a steady external flow. For unsteady external flow we have: $\frac{\partial u_e}{\partial t} = c\frac{\partial \delta^*}{\partial t} + \frac{\partial}{\partial t}\left(u_{ext} - c\delta^*_{ext}\right)$.

If the system of equations becomes singular, the determinant of one of the matrices is zero. For the models used here, matrix $[Q]$ has this possibility.

$$[Q]_{lam} = \begin{bmatrix} \frac{c}{u_e}(2\theta + \delta^*) & 1 \\ \frac{\mathrm{d}H^*}{\mathrm{d}H} + 3c\frac{\delta^k}{u_e} & -\frac{\mathrm{d}H^*}{\mathrm{d}H}\frac{\delta^*}{\theta^2} \end{bmatrix}; \qquad [Q]_{turb} = \begin{bmatrix} \frac{1}{H} + \frac{c\delta^*}{u_e}(1 + \frac{2}{H}) & -\frac{\delta^*}{H^2} \\ \frac{H_1}{H}(1 + \frac{c\delta^*}{u_e}) & \frac{\delta^*}{H}\left(\frac{\mathrm{d}H_1}{\mathrm{d}H} - \frac{H_1}{H}\right) \end{bmatrix}. \tag{16}$$

The singularity is possible for matrix $[Q]$ in cases without the quasi-simultaneous interaction. This can easily be seen from the expressions of $[Q]$ with the interaction law coefficient set to zero. Then $[Q]$ becomes singular at the point of separation where $\frac{\mathrm{d}H^*}{\mathrm{d}H} = 0$ and $\frac{\mathrm{d}H_1}{\mathrm{d}H} = 0$, which is the case for the models used here for H^* and H_1.

However, in the interaction-law equation the coefficient is always positive ($c = \frac{4}{\pi h}$) and therefore the singularity is removed: $\det[Q] > 0$. The result of a large enough positive interaction coefficient is that the quasi-simultaneous interaction method should be able to calculate separated flows.

4.4 Characteristic variables

The previous analyses have been expressed in primary variables (u_e, δ^*, H, etc.) and the equations in the set are coupled. Using characteristic variables - obtained from primary variables via a transformation - gives insight in the characteristic directions of the flow and decouples the equations. This is needed for some discretisation schemes that require the local direction of the flow. For 2D applications the sign of the eigenvalues is an indication of the characteristic direction. In this application, the eigenvalues are always positive due to the interaction-law[3].

Another main advantage of using a set of equations in characteristic variables is that the equations in the decoupled system can be solved separately. The eigenvalues need to be determined and from that a transformation matrix S is constructed containing the eigenvectors. The transformation that we apply is:

$$S\psi = \phi, \quad S\frac{\partial \psi}{\partial x} = \frac{\partial \phi}{\partial x} \quad \left(\frac{\partial S}{\partial x} = 0\right). \tag{17}$$

By multiplying the system with $[P]^{-1}$, applying the transformation of equation (17) and subsequently multiplying with $[S]^{-1}$ we end up with:

$$[P]\frac{\partial \phi}{\partial t} + [Q]\frac{\partial \phi}{\partial x} = \{R\} \quad \Rightarrow \quad \frac{\partial \psi}{\partial t} + [\Lambda]\frac{\partial \psi}{\partial x} = [S]^{-1}[P]^{-1}\{R\}, \quad [\Lambda] = [S]^{-1}[P]^{-1}[Q][S] \tag{18}$$

and $[\Lambda] = diag(\lambda_1, \lambda_2)$. The equations in the set are now decoupled. As the systems with primary and characteristic variables are analytically equal, simulations with both sets should yield equal results. In the next section it is shown that this is indeed the case.

5 Results

Simulations of attached and separated flows for laminar and turbulent boundary-layer flows have been carried out. The aim is to show that the quasi-simultaneous interaction method is able to handle both attached and separated flows. Furthermore, the simulations have been run with the equations expressed in primary and characteristic variables. The equations used for the simulations in primary variables are those given in section 4.1 and the simulations with characteristic variabels use equation (18). The equations are discretised using an upwind scheme in space and a backward-Euler discretisation in time. Table 1 shows other parameters for the simulations.

[3] The eigenvalues can be computed by finding the roots (λ_1, λ_2) of the characteristic equation that follows from $\det[P\lambda - Q] = 0$. The product of the eigenvalues is determined by $\lambda_1\lambda_2 = \frac{\det[Q]}{\det[P]}$.

	Laminar	Turbulent
Reynolds number	1.0×10^5	11.5×10^5
Δ x	1/240	1/240
Δ t	1000 (flat plate) 1 with 1000 time-steps (dented plate)	1000
x-range	0.5 - 1.5	0.0-1.0
dent depth (% of plate length)	3	5

Table 1: Parameters used for simulations.

5.1 Laminar case

The result of simulations of flow over over a flat plate is shown in Figure 5. The flow is attached. Plots of δ^*, H and the skin-friction coefficient with respect to the x-coordinate are presented.

Figure 6 shows the results of a laminar flow over a dented plate. Separation occurs in the dent. This can be concluded from Figure 6c where the skin-friction coefficient becomes negative.

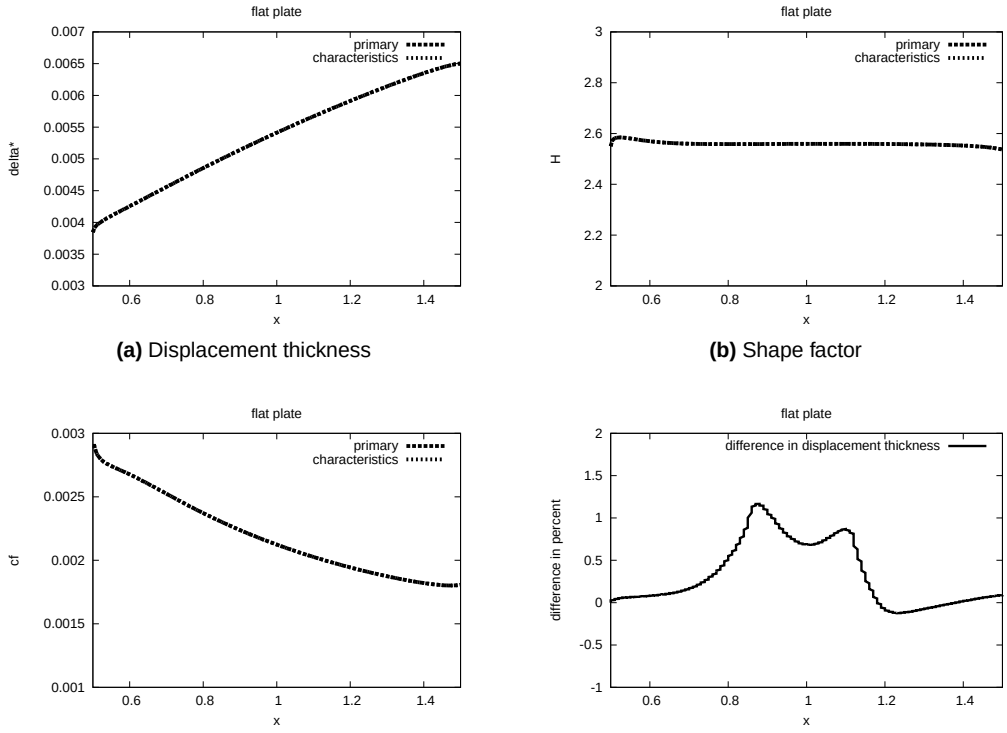

(a) Displacement thickness

(b) Shape factor

(c) Skin-friction

(d) Difference in % in δ^*

Figure 5: Attached laminar boundary-layer flow over a flat plate with $x \in [0.5; 1.5]$, $\Delta x = 1/240$, $Re = 10^5$, $\Delta t = 1000$, 1 time-step.

For both geometries (i.e. flat and dented plate), simulations with primary and characteristic variables have been performed. It can be observed from Figures 5 and 6 that the results are on top of each other. Figures 5d and 6d show the differences in displacement thickness between the simulations with primary and characteristic variables. These differences are less than one percent and based on that we conclude that the choice of variables has negligible influence on the converged result.

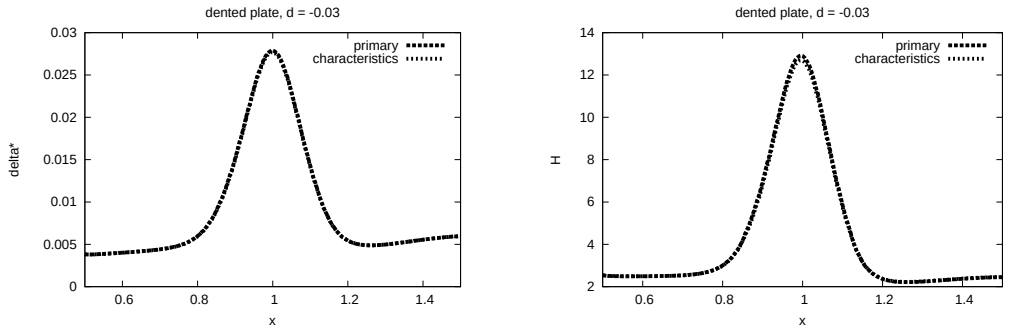

(a) Displacement thickness **(b)** Shape factor

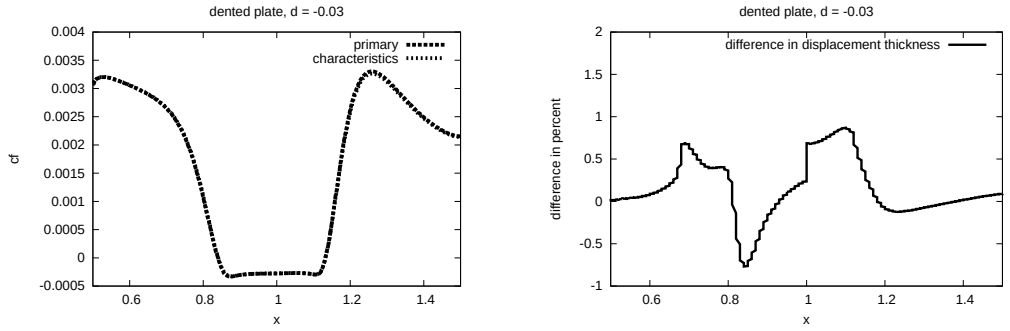

(c) Skin-friction **(d)** Difference in % in δ^*

Figure 6: Separated laminar boundary-layer flow over a dented plate with $x \in [0.5; 1.5]$, $\Delta x = 1/240$, $Re = 10^5$, $\Delta t = 1$, 10^4 time-steps.

5.2 Turbulent case

For the turbulent boundary-layer model, simulations on a flat and dented plate have been performed as well. Figure 7 shows the results for flow over a flat plate for simulations carried out with primary and characteristic variables. The flow is attached. The results of simulations with primary and characteristic variables coincide. Figure 7d shows that the difference in displacement thickness is zero for the two simulations carried out.

Results for flow over a dented plate are presented in Figure 8. It follows from Figure 8c that the flow is separated in the dent. From Figure 8 we conclude that for separated, turbulent flows, the use of primary and characteristic variables yield the same result.

6 Conclusion

The quasi-simultaneous interaction method has been applied to two-dimensional boundary-layer flows over flat and dented plates. Both laminar and turbulent boundary-layer flows have been investigated. It has been shown that the method can handle large separated flows. Furthermore, from simulations of flows over flat and dented plates it could be concluded that the use of primary and characteristic variables converge to the same result for all cases investigated.

Future tests of the implementation of the interaction-law will include the simulation of flows over airfoils.

Acknowledgements The authors would like to thank the other members of the ECN Wind Energy ROTORFLOW project team for the support and fruitful discussions. The financial support by the ministry of Economical Affairs of The Netherlands is gratefully acknowledged. This research is carried out under contract of the InnWind project of SenterNovem (Agentschap NL).

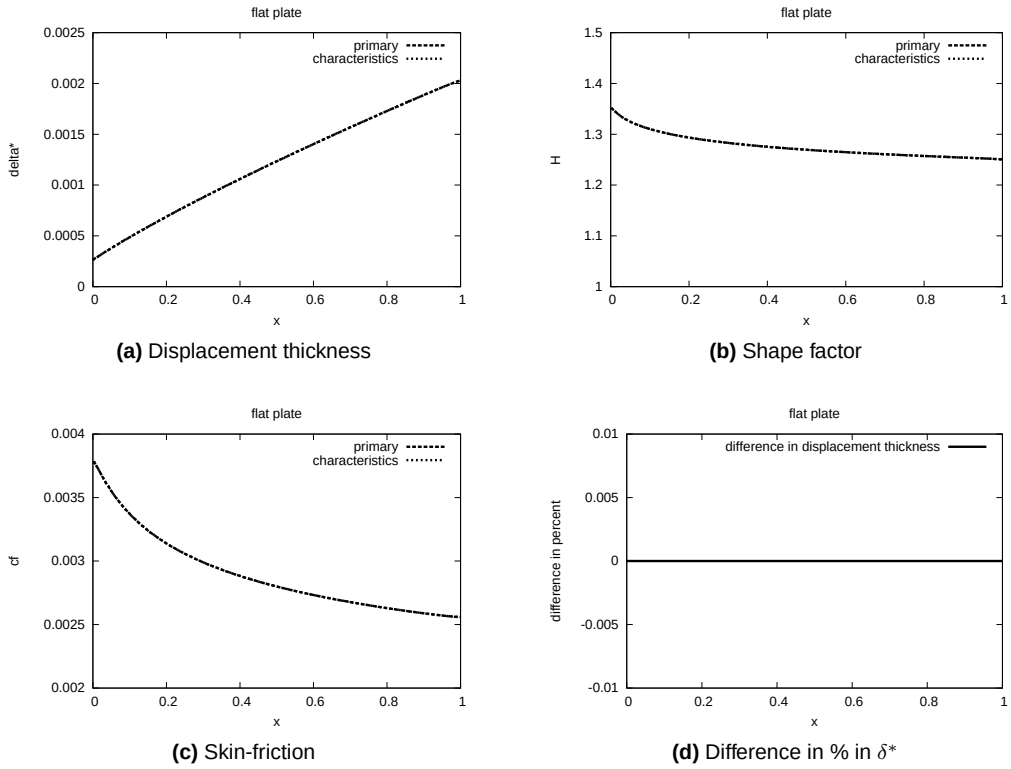

(a) Displacement thickness

(b) Shape factor

(c) Skin-friction

(d) Difference in % in δ^*

Figure 7: Attached turbulent boundary-layer flow over a flat plate with $x \in [0.0; 1.0]$, $\Delta x = 1/240$, $Re = 11.5^5$, $\Delta t = 1000$, 1 time-step.

References

[1] D. Catherall and K.W. Mangler. The integration of the two-dimensional laminar boundary-layer equations past the point of vanishing skin friction. *Journal of Fluid Mechanics*, 26:163–182, 1966.

[2] M. Drela. XFOIL: An analysis and design system for low Reynolds number airfoils. *Low Reynolds Numbers Aerodynamics*, 1989.

[3] D.E. Edwards. Analysis of three-dimensional flow using interacting boundary-layer theory. In F.T. Smith and S.N. Brown, editors, *Proc. IUTAM Symposium on boundary-Layer separation*, pages 163–178, 1987.

[4] S. Goldstein. On laminar boundary layer flow near a point of separation. *Quart J Mech Appl Math*, 1:43–69, 1948.

[5] M.R. Head. Entrainment in the turbulent boundary layer. Technical report, Aeronautical Research Council R&M 3152, 1960.

[6] R. Houwink and A.E.P. Veldman. Steady and unsteady flow computations for transonic airfoils. *AIAA*, 84-1618, 1984.

[7] B.A. Nishida. *Fully Simultaneous Coupling of the Full Potential Equation and the Integral Boundary Layer Equations in Three Dimensions*. PhD thesis, Massachusetts Institute of Technology, USA, 1996.

[8] H. Özdemir. Development of a discontinuous Galerkin method for the unsteady integral boundary layer equations. In *8th Euromech Fluid Mechanics Conference, Bad Reichenhall, Germany*, September 13-16, 2010.

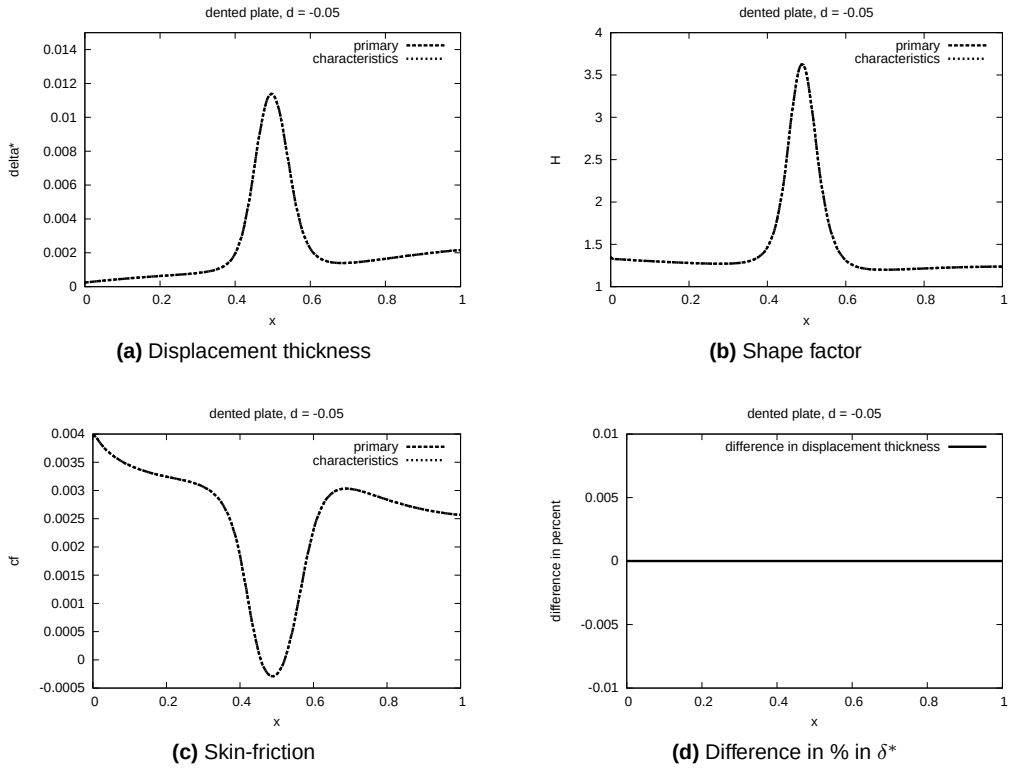

(a) Displacement thickness

(b) Shape factor

(c) Skin-friction

(d) Difference in % in δ^*

Figure 8: Separated turbulent boundary-layer flow over a dented plate with $x \in [0.0; 1.0]$, $\Delta x = 1/240$, $Re = 11.5^5$, $\Delta t = 1000$, 1 time-step.

[9] H. Schlichting and K. Gersten. *Boundary Layer Theory, 8th Revised and Enlarged Edition*. Springer-Verlag, 1999.

[10] A.J. van der Wees and J. van Muijden. A robust quasi-simultaneous interaction method for a full potential flow with a boundary layer with application to wing/body configurations. In *Proceedings of the 5th symposium on numerical and physical aspects of aerodynamic flows*, 1992.

[11] A.E.P. Veldman. New, quasi-simultaneous method to calculate interacting boundary layers. *AIAA Journal*, 19:79–85, 1981.

[12] A.E.P. Veldman. A simple interaction law for viscous-inviscid interaction. *Journal of Engineering Mathematics*, 65:367–383, 2009.